Since January 2020 Elsevier has created a COVID-19 resource centre with free information in English and Mandarin on the novel coronavirus COVID-19. The COVID-19 resource centre is hosted on Elsevier Connect, the company's public news and information website.

Virus Research 167 (2012) 207–218

Contents lists available at SciVerse ScienceDirect

Virus Research

journal homepage: www.elsevier.com/locate/virusres

The R-rich motif of *Beet black scorch virus* P7a movement protein is important for the nuclear localization, nucleolar targeting and viral infectivity

Xiaohui Wang, Yanjing Zhang, Jin Xu, Lindan Shi, Huiyan Fan, Chenggui Han, Dawei Li, Jialin Yu*

State Key Laboratory of Agro-Biotechnology, College of Biological Sciences, China Agricultural University, Beijing 100193, PR China

ARTICLE INFO

Article history:
Received 4 December 2011
Received in revised form 1 May 2012
Accepted 6 May 2012
Available online 22 May 2012

Keywords:
Beet black scorch virus
P7a
Nuclear localization
Importin α
Fibrillarin
Viral infectivity

ABSTRACT

Beet black scorch virus (BBSV) encodes three movement proteins (P7a, P7b and P5′) that facilitate its cell-to-cell movement. An arginine-rich motif of P7a N-terminus was found to determine nuclear and nucleolar localization. Amino acids substitution or deletion of the R-rich motif interfered with P7a nuclear and nucleolar localization. Bimolecular fluorescence complementation (BiFC) assays revealed that P7a protein interacted with *Nicotiana benthamiana* nuclear import factor importin α, suggesting that P7a is translocated into the nucleus by the classical importin α/β-dependent pathway. Moreover, P7a also interacted with the nucleolar protein fibrillarin. Mutations in the R-rich motif of P7a diminished P7a interactions with importin α and fibrillarin, influenced viral replication in *Nicotiana benthamiana* protoplasts and altered the symptom phenotype and viral RNA accumulation in *Chenopodium amaranticolor* plants. These results demonstrate that the R-rich motif of P7a is correlated with nuclear and nucleolar localization, viral replication and virus infection.

1. Introduction

The nuclear localization proteins normally require successful translocation through the nuclear pore complex (NPC) (Cronshaw et al., 2002; Krichevsky et al., 2006). Although the nuclear pore complexes allow small spontaneous proteins(<60 kD) to enter the nuclear, many proteins contain nuclear localization signals (NLS) to facilitate their transport (Kosugi et al., 2009; Krichevsky et al., 2006; Lange et al., 2007). Classical NLS have either one (monopartite) or two (bipartite) basic amino acid motifs composed of arginines and lysines (Lange et al., 2007). A monopartite NLS, as exemplified by the SV40 large T antigen NLS, is composed of at least four consecutive basic amino acids (PKKKRRV) (Kalderon et al., 1984); whereas bipartite NLS signals, similar to the nucleoplasm protein NLS (KRPAATKKAGQAKKK), contain two basic amino acid clusters separated by a 10–12 amino acid spacer (Robbins et al., 1991). The nucleocytoplasmic transport model is best understood as the nuclear importin α/β pathway (Lange et al., 2007; Truant and Cullen, 1999). During import *via* the importin α/β pathway, the importin α protein binds to cytoplasmic proteins that contain NLS, and couples the proteins to importin β proteins (Adam and Geracet, 1991; Kosugi et al., 2009; Weis et al., 1996). Importin β next docks the trimeric cargo-import-α/β complex to the NPC and then releases the cargo into the nucleus *via* binding of Ran-GTP (Lange et al., 2007; Pemberton and Paschal, 2005; Weis, 2003). Some viral proteins that contain a classical NLS were defined to follow this nuclear import pathway and interact first with importin α (Greber and Fassati, 2003; Guerra-Peraza et al., 2005; Truant and Cullen, 1999).

Some available reports suggest that the nuclear proteins encoded by the plant RNA virus which replicate in cytoplasm interact with the nuclear elements or suppress host defense. For example, the P19 suppressor protein of *Tomato bushy stunt virus* interacts with the ALY proteins in nucleus for regulation of suppressor activity (Canto et al., 2006; Uhrig et al., 2004). Only a few plant viral proteins localize to the nucleolus, which is a prominent sub-nuclear compartment for processing rRNA transcripts and pre-rRNAs, and biogenesis of pre-ribosomal particles, as well as stress response activities, gene silencing and cell cycle regulation (Boisvert et al., 2007; Olson, 2004; Olson et al., 2000; Pontes et al., 2006). Interestingly, the *Groundnut rosette virus* (GRV) ORF3 protein and *Potato virus A* (PVA) NIa–VPg protein accumulate in the nucleolus and Cajal bodies (CBs), and they also interact with the nucleolar protein fibrillarin (Kim et al., 2007a,b; Rajamaki and Valkonen, 2009; Ryabov et al., 2004). GRV ORF3 protein interacts with fibrillarin to form a ribonucleoprotein (RNP) that facilitates the long-distance movement and systemic infection of the virus (Canetta et al., 2008; Kim et al., 2007a,b). However, the VPg-fibrillarin interaction influences nucleolar functions and suppression of host gene silencing (Rajamaki and Valkonen, 2009).

Beet black scorch virus (BBSV) which is a member of the genus *Necrovirus* (Lommel et al., 2005), was first identified in China (Cao

* Corresponding author. Tel.: +86 10 62732875; fax: +86 10 62732012.
E-mail address: yjl@cau.edu.cn (J. Yu).

0168-1702/$ – see front matter © 2012 Elsevier B.V. All rights reserved.
http://dx.doi.org/10.1016/j.virusres.2012.05.001

et al., 2002), and has subsequently been found in Iran, North America and Europe (Autonell et al., 2006; Gonzalez-Vazquez et al., 2009; Koenig and Valizadeh, 2008; Weiland et al., 2006). The virus infects sugar beet plants and produces black scorched leaves and necrotic fibrous roots (Cai et al., 1999; Jiang et al., 1999). Sequence analyses of BBSV strains have revealed that the genome, which encodes 6 proteins, shares the highest nucleotide sequence identity (61%) with *Tobacco necrosis virus D* (Cai et al., 1999; Cao et al., 2002). The 5′-proximal ORFs, P23 and its read-through P82, which are expressed directly from the viral RNA, encode RNA polymerase subunits (Yuan et al., 2006). The p24 coat protein (CP), which is encoded by sgRNA2, localizes to the nucleus (Zhang et al., 2011) and is involved in long-distance movement during systemic infection of *N. benthamiana* and plays a role in eliciting various leaf symptom phenotypes (Cao et al., 2006). However three small ORFs (P7a, P7b and P5′) expressed from sgRNA1 are located in the central region of the BBSV genome and these proteins appear to be dedicated cell-to-cell movement proteins (Yuan et al., 2006). Moreover, the BBSV movement strategy employs the coordinated actions of P7a, P7b and P5′, and the coat protein is not required for cell-to-cell movement (Cao et al., 2006; Yuan et al., 2006).

The BBSV P7a may have other functions as the first movement protein of some other viruses (Morozov and Solovyev, 2003; Wright et al., 2010). In this study, fluorescent BBSV movement protein P7a was expressed transiently in *N. benthamiana* leaf cells *via Agrobacterium* infiltration to determine cellular localization. We also performed mutational experiments to identify the nuclear localization signal of P7a and to determine whether mutant of R-rich motif influenced the viral replication and infection. The results revealed that the R-rich motif of P7a N-terminal determined the P7a nuclear localization, and was required for viral replication and infectivity.

2. Materials and methods

2.1. Construction of mutant BBSV cDNAs

Recombinant BBSV cDNA clones were constructed based on a plasmid vector (Fig. 1A) containing the full-length infectious cDNA clone of BBSV (pUBF52) (Yuan et al., 2006). Mutations were introduced into the P7a coding sequence to substitute basic residues with alanines in arginine-rich motifs (Fig. 1B). Site-directed mutagenesis of the P7a coding sequence was performed in the plasmid pUBF52 by an overlap extension PCR procedure using self-complementary primers (Table 1) (Urban et al., 1997). The deletion mutant pUBF-P7a$_{\Delta R5\text{-}K22}$ in which the residues ^{5}RSEQRRERRVRSRSEDRK^{22} were excised, was created by inverse PCR. The cDNA clone mutants were verified by sequencing.

2.2. Transient expression of fused fluorescent protein in plant leaves by agroinfiltration

For transient protein expression in leaves by agroinfiltration, binary vectors constructed in these studies were derived from the pGD plasmids (pGDG and pGDR) (Goodin et al., 2002). To construct pGDG-MP, the MP coding region was amplified from the corresponding infectious BBSV cDNA by PCR with correct primers (Table 1). The PCR products were then inserted into the binary pGDG plasmid and the recombinant plasmids were verified by sequencing. To prepare pGDR-GUS derivatives for reporter analysis, a DNA fragment containing the full-length GUS gene sequence was PCR amplified from P26-GUS (From our lab) using specific primers (Table 1). The PCR fragment was cloned into the pGDR vector to yield the plasmid pGDR-GUS (Fig. 1E). The pGDR-GUS-P7a and pGDR-GUS-P7a mutant plasmids were constructed by amplifying the BBSV cDNA clones using specific primers (Table 1) for each mutant and cloned into vector pGDR-GUS. The constructs were verified by sequencing.

Binary vectors were transformed into the *Agrobacterium tumefaciens* strain EHA105 and *Agrobacterium* infiltrations of *N. benthamiana* leaves were performed essentially as described by Johansen and Carrington (2001). The *Agrobacterium* mixtures also usually included bacteria containing the pGD-P19 plasmid to minimize host gene silencing (Zhang et al., 2011).

2.3. BiFC assays for subcellular localization of BBSV P7a by confocal microscopy

The adaptor protein importin α (Kanneganti et al., 2007) and the *N. benthamiana* fibrillarin genes were amplified by PCR using appropriate primers (Table 1) and cloned into the binary expression cassette pSPYNE-35S (Walter et al., 2004) to generate pYN-importin α and pYN-Fib (Fig. 1F). The P7a coding sequence and relevant mutants were cloned in-frame into pSPYCE-35S (Walter et al., 2004). The resulting binary vectors were transfected into the *A. tumefaciens* strain EHA105, and the *Agrobacterium* cultures were grown and resuspended as described by Zhang et al., (2011). To suppress possible host gene silencing activities, the pNE and pNC cultures were combined with pGD-P19 at a (*V*/*V*) ratio of 0.5:0.5:0.3 (pNE:pCE:P19), and BiFC assays were carried out at 2–3 days after agroinfiltration of *N. benthamiana* leaves.

Samples of *N. benthamiana* leaves expressing GFP or RFP fusion proteins or those expressing YFP fluorescence resulting from BiFC were visualized by confocol laser scanning microscopy using a Nikon ECLIPSE TE2000-E microscope. GFP/YFP was visualized using the 488 nm line of an Argon laser with an emission filter BP505-530 on the PMT detector. RFP was excited using a 543 nm laser and imaged using the META detector set for 570–600 nm. DAPI fluorescence was excited with a filter set consisting of an emission filter of 435–485 nm and a 408 nm laser. The images were captured and processed with a Nikon ECLIPSE TE2000-E microscope, processed with ECLIPSE EZ-C1 3.00 FreeViewer software (Nikon Corporation) and data was captured as single optical sections.

2.4. Analysis of BBSV RNA by inoculation of C. amaranticolor with the in vitro transcripts

BBSV plasmids driven by a T7 promoter were linearized with *Sma*I and used as templates for transcription *in vitro* at 37 °C for 1hr with a T7 RNA polymerase kit as described by the manufacturer (Promega). For mechanical inoculation, RNAs synthesized *in vitro* were diluted with an equal volume of inoculation buffer (50 mM glycine, 30 mM K_2HPO_4, 1% bentonite, 1% celite, pH 9.2), rubbed onto young *C. amaranticolor* leaves, and then inoculated plants were placed in a growth chamber at 18 °C. Total RNA was extracted from the inoculated leaves (Yuan et al., 2006), and was used for northern blot analysis. A cDNA probe complementary to 900 nt (2647–3543 nt) at the 3′-proximal of the BBSV genome was used to assess the BBSV RNA amount. The ^{32}P-α-labeled probes were prepared by the prime-α-gene labeling system according to the manufacturer's (Promega) instructions (Yuan et al., 2006).

2.5. Protoplast transfection and Northern blot of viral RNA

Mesophyll protoplasts were isolated from the leaves of *N. benthamiana* plants (Nagy and Maliga, 1976). Approximately 10^6 freshly isolated protoplasts were transfected with 20 μg of recombinant viral transcripts with a PEG-calcium-mediated transfection method followed by an 18-h viral replication period (Yoo et al.,

Fig. 1. Diagram of the BBSV genome and p7a mutants, and the binary vectors used for transient expression of fusion proteins. (A) Infectious BBSV cDNA clone showing the coding regions. (B) P7a protein mutants created by site-directed mutagenesis of the N-terminal arginine-rich motif or deletions within the motif. (C) Four pGDG vectors used to assess subcellular localization of C-terminal GFP fusions to the P7a, P7b and P5′ movement protein genes, and a fibrillarin gene. (D) A pGDR-Fib vector used as a reporter for nucleolar localization of a fibrillarin gene. (E) P7a gene or P7a mutants fused downstream of the *GUS* sequence in pGDR to assess nuclear localization. (F) Insertion of fibrillarin or importin α into pSPYNE-35S for Bi-molecular fluorescence complementation (BiFC) assays. (G) P7a gene and mutants insertions into pSPYCE-35S for BiFC analyses.

2007). Total RNA was extracted from the transfected protoplasts using Trizol (Invitrogen) and used for northern blot analysis.

3. Results

3.1. Subcellular localization of the Beet black scorch virus movement proteins

Our previous studies revealed that three small, centrally located ORFs within the BBSV genome are each required for cell-to-cell movement in susceptible hosts (Yuan et al., 2006). Because of our inability to determine the subcellular localization of the movement proteins by immunolocalization, the coding sequences of P7a, P7b and P5′ were fused in-frame to the 3′-end of *gfp* in the binary vectors of pGDG (Fig. 1C).The GFP:MP fusions were co-expressed ectopically by agro-infiltration in *N. benthamiana* leaves. After two to three days of incubation, the infiltrated leaves were fixed, stained with 4′6′-diamidino-2-phenylindole (DAPI) and examined by laser confocal scanning microscopy. Confocal microscopy of *N. benthamiana* epidermal cells of the infiltrated leave revealed that a predominant proportion (84%) of the pGDG-P7a fluorescence accumulated in the nucleus, where it co-localized with the DAPI signal and that the remaining proportion of the fluorescence appeared in the cytoplasm and at the cell wall (Fig. 2A). In marked contrast, pGDG-P7b and pGDG-P5′ failed to exhibit nuclear fluorescence and instead localized almost in the cytoplasm (98%) and at the cell wall (Fig. 2B and C). As a consequence of its small size and ability to diffuse into the nucleus, GFP localized in both the cytoplasm and the nucleus when expressed alone (Fig. 2D). These results show that P7a has nuclear localization properties, whereas the P7b and P5 proteins are restricted to the cytoplasm and the cell wall.

3.2. A short arginine-rich peptide motif mediates P7a nuclear localization

Although the P7a protein does not harbor a classical NLS as predicted by the database (http://cubic.bioc.columbia.edu/predictprotein), the N-terminus of P7a includes an arginine (R)-rich motif residing between amino acids 5–22 (^{5}RSEQRRERRVRSRSEDRK^{22}). In order to prevent the RFP reporter protein from spontaneous movement into the nucleus due to its small size, a 68.4 kDa GUS protein was inserted between the RFP protein and the full-length BBSV P7a protein, and the resulting RFP-GUS-P7a protein also can localize in the nucleus (Fig. 3A). To determine the requirement of the N-terminal 18 amino acids domain for nuclear targeting of BBSV P7a, the nucleotide sequence corresponding to the (^{5}RSEQRRERRVRSRSEDRK^{22}) fragment was deleted to form the construct pGDR-GUS-P7a$_{\Delta R5\text{-}K22}$ (Fig. 1E). The nuclear accumulation of the mutated protein was reduced

Table 1
Clones and oligonucleotides used in localization, interaction, and infectivity.

Clone	Primer	5′–3′ oligo sequence[b]
pGDG-P7a	P7a *Xho*IF[a]	CCGCTCGAGCTATGGAACAACAGCGTAGTGAAC
	P7a *Bam*HIR	CGCGGATCCGAAGTGGAAATGTTGTGTAAACTC
pGDG-P7b	P7b *Xho*IF	CGCGGATCCGAAGTGGAAATGTTGTGTAAACTC
	P7b *Bam*HIR	CGCGGATCCGTTCGTGGAAACTTTACTAGTGG
pGDG-P5′	P5′XhoIF	CCGCTCGAGCTATGTCGTACAGGAGAAGCCCTC
	P5′ *Bam*HIR	GCGGATCCTGTATTGCGTCTTCTGATTGTTTTCGTG
Amplification of BBSV_P7afull or BBSV_P7a mutants, and the mutants of BBSV CDNA clones		
pGDR-GUS-P7a	P7a *Sal*IF	ACGCGTCGACATGGAACAACAGCGTAGTGAACAAC
pGDR-GUS-P7a$_{R9A,R10A}$	P7a *Bam*HIR	CGCGGATCCGAAGTGGAAATGTTGTGTAAACTC
pGDR-GUS-P7a$_{R12A,R13A}$		
pGDR-GUS-P7a$_{R15A,R17A}$		
pGDR-GUS-P7a$_{R21A,K22A}$		
pGDR-GUS-P7a$_{R5A}$	P7a N mutant *Sal*IF	ACGCGTCGACATGGAACAACAGgcTAGTGAACAACG
	P7a *Bam*HIR	CGCGGATCCGAAGTGGAAATGTTGTGTAAACTC
pGDR-GUS-P7a$_{\Delta R5\text{-}R22}$	P7a R-rich delete *Sal*IF	ACGCGTCGACATGGAACAACAGTCTATGTCTGATGTAGGGCAATC
	P7a *Bam*HIR	CGCGGATCCGAAGTGGAAATGTTGTGTAAACTC
pYC-P7a	P7a *Bam*HIF	CGGGATCCATGGAACAACAGCGGAGTGAAC
pYC-P7a$_{R9A,R10A}$	P7a *Xho*IR	CCGCTCGAGGAAGTGGAAATGTTGTGTAAACTC
pYC-P7a$_{R12A,R13A}$		
pYC-P7a$_{R15A,R17A}$		
pYC-P7a$_{R21A,K22A}$		
pYC-P7a$_{R5A}$	P7a N mutant *Bam*HIF	CGCGGATCCATGGAACAACAGgcTAGTGAACAACG
	P7a *Xho*IR	CCGCTCGAGGAAGTGGAAATGTTGTGTAAACTC
pYC-P7a$_{\Delta R5\text{-}R22}$	P7a R-rich delete *Bam*HIF	GCGGATCCATGGAACAACAGTCTATGTCTGATGTAGGGCAATC
	P7a *Xho*IR	CCGCTCGAGGAAGTGGAAATGTTGTGTAAACTC
pUBF-P7a$_{R5A}$	F(BBSV 2228–2254)	ATGGAACAACAGgcTAGTGAACAACG
	R(BBSV 2228–2254)	CGTTGTTCACTAgcCTGTTGTTCCAT
pUBF-P7a$_{R9A,R10A}$	F(BBSV 2240–2269)	CGTAGTGAACAAgcTgcTGAGCGTAGAGTG
	R(BBSV 2240–2269)	CACTCTACGCTCAgcAgcTTGTTCACTACG
pUBF-P7a$_{R12A,R13A}$	F(BBSV2249–2277)	CAACGTCGTGAGgcTgcAGTGAGAAGTAG
	R(BBSV2249–2277)	CTACTTCTCACTgcAgcCTCACGACGTTG
pUBF-P7a$_{R15A,R17A}$	F(BBSV 2262–2290)	GTAGAGTGgcAAGTgcATCGGAGGACAGG
	R(BBSV 2262–2290)	CCTGTCCTCCGATgcACTTgcCACTCTAC
pUBF-P7a$_{R21A,K22A}$	F(BBSV 2276–2313)	AGATCGGAGGACgcGgcGTCTATGTCTTGGATG
	R(BBSV 2276–2313)	CATCAGACATAGAgcCgcCGTCCTCCGATCT
pUBF-P7a$_{\Delta R5\text{-}K22}$	F(BBSV2291–2323)	TCTATGTCTGATGTAGGGCAATCTGCTGTC
	R(BBSV 2214–2239)	CTGTTGTTCCATGAAAAGTGGTTAGG
Amplification of other full-length genes used in the study		
pGDR-Fib/pGDG-Fib	Fib *Xho*IF	CCGCTCGAGCTATGGTTGCACCAACTAGAGGTCGCG
	Fib *Bam*HIR	CGCGGATCCGGCAGCAGCCTTCTGCTTCTTCGG
pYN-Fib	Fib *Bam*HIF	CGCGGATCCATGGTTGCACCAACTAGAGGTCGCG
	Fib *Xho*IR	CCGCTCGAGGGCAGCAGCCTTCTGCTTCTTCGG
pGDR-GUS	GUS *Xho*IF	CCGCTCGAGCTATGTTACGTCCTGTAGAAACCCCAAC
	GUS *Sal*I R	ACGCGTCGACTTGTTTGCCTCCCTGCTGCGGTTTTTC
pYN-importin α	imp *Bam*HIF	GCGGGATCCATGTCGCTGAGGCCGAATTCGAGAAC
	imp *Xho*IR	GCGCTCGAGTGAACTGAAGTTGAATCCTCCTGATG

aa, amino acid.
Lowercase characters indicating the replaced nucleic acids.
[a] F, forward primer; R, reverse primer.
[b] Restriction sites are underlined.

to barely detectable levels compared to the wild-type pGDR-GUS-P7a reporter derivative, which again exhibited pronounced nuclear fluorescence (Fig. 3A and B). To investigate whether R-rich residues within the BBSV P7a domain are responsible for nuclear localization, a series of mutants were constructed the plasmid pUBF-P7a in which arginine residues were substituted for alanine residues (Fig. 1B). The localization of mutants pGDR-GUS-P7a$_{R5A}$, pGDR-GUS-P7a$_{R9A,R10A}$ and PGDR-GUS-P7a$_{R21A,K22A}$ was comparable to that of pGDR-GUS-P7a in that red fluorescence accumulated in both the nucleus and in the cytoplasm (Fig. 3C, D and G). However, the double P7a mutants pGDR-GUS-P7a$_{R12A,R13A}$ or pGDR-GUS-P7a$_{R15A,R17A}$ exhibited cytoplasmic fluorescence due to exclusion of the fusion protein mutants from the nucleus (Fig. 3E and F). The control vector pGDR-GUS displayed red fluorescence in the cytoplasm and in the cell wall (Fig. 3H) and intracellular localization of the RFP-P7a mutant fusion proteins was confirmed by DAPI staining using fluorescein. These results strongly suggest that the ^{12}RRVRSR^{17} residing in the N-terminus of R-rich motif P7a is critical for nuclear localization.

3.3. The R-rich motif interferes with the interaction with P7a and the nuclear import protein

Although the R-rich motif is not a classical NLS, we investigated whether P7a interacts with the importin α protein for nuclear entry. The importin α gene from *N. benthamiana* was cloned into pYN-importin α (Fig. 1F) and P7a or P7a mutants cloned into pYC-7a (Fig. 1G) in bimolecular fluorescence complementation assays (BiFC) (Walter et al., 2004). Within two to three days after agroinfiltration of bacteria cells containing the YN-Importin α and YC-P7a fusions into *N. benthamiana* leaves, epidermal cells exhibited a strong fluorescent signal that was concentrated in the nucleus (Fig. 4A). Fluorescence was also observed in the nuclei when pYN-importin α was co-infiltrated with mutants pYC-P7a$_{R5A}$ (Fig. 4B) or pYC-P7a$_{R21A,K22A}$ (Fig. 4D). In contrast, confocal microscopy of the agroinfiltrated epidermal cells co-expressing pYC-P7a$_{R12AR13A}$, pYC-P7a$_{R15AR17A}$ or pYC-P7a$_{\Delta R5\text{-}K22}$ with pYN-importin α failed to exhibit nuclear fluorescence (Fig. 4E). However, weak fluorescence was observed in the nuclei of leaf cells agroinfiltrated with the

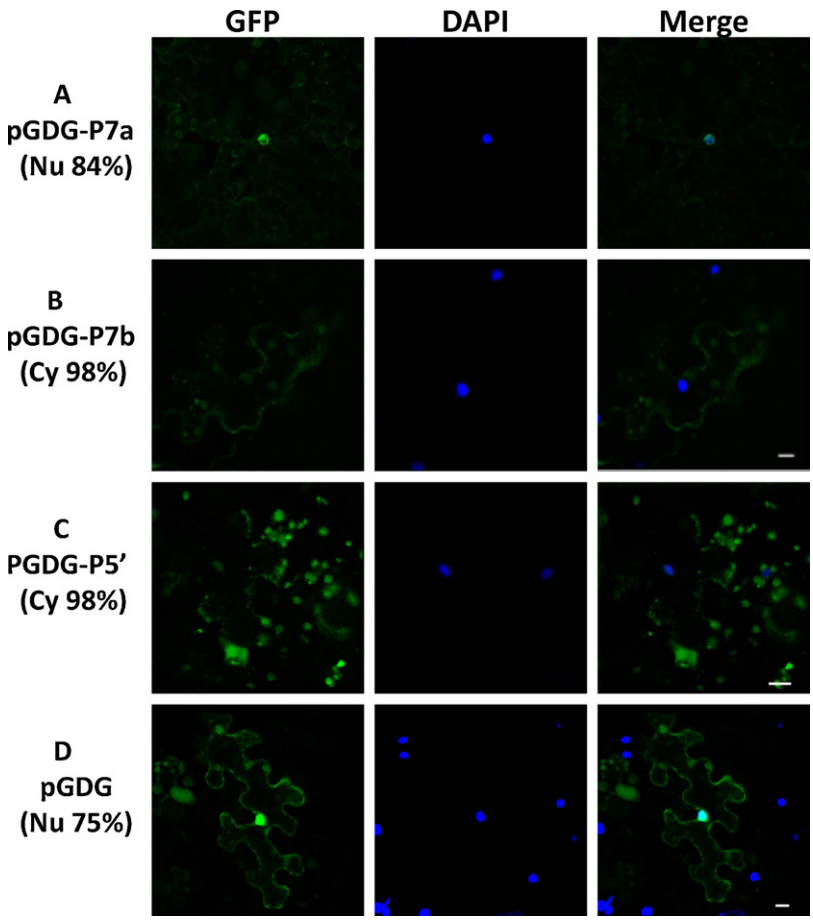

Fig. 2. Subcellular localization of BBSV P7a, P7b and P5′ by fluorescence microscopy of GFP expressed from pGDG vectors in *N. benthamiana*. Epidermal leaf cells agroinfiltrated with (A) pGDG-7a, (B) pGDG-7b, or (C) pGDG-P5′ vectors for transient expression of fusion proteins. (D) The pGDG binary vector expressing only GFP was infiltrated in parallel as a control, and DAPI (4′,6-diamidino-2-phenylindole) was used for nuclear staining of leaf cell. *Note*: The ratios shown in parentheses beside each treatment indicate the percentage of GFP fluorescence estimated to be localized in the nuclei (Nu) or the cytoplasm (Cy). A total 100 epidermal cells of *N. benthamiana* in which GFP fluorenscence were detected in the cells were examined in nuclear or in cytoplasm by fluorescence microscopy 2–3 days. And the experiment were repeated for three times. Bars = 10 μm.

plasmids pYC-P7a$_{R9A,R10A}$ and pYN-importin α (Fig. 4C). To study the interaction using an *in virto*-binding method, far-western analysis was used (Wu et al., 2007). The His-labeled P7a was purified from *E. coli* and importin α was fused to GST-tag. Blots containing GST-importin α and GST protein was incubated with purified His-labeled P7a, and visualized by anti-His antibodies. The results show that the His-labeled P7a was able to bind the GST-Importin α (Supplementary material Fig. S1). Taken together, these results indicate that the P7a ^{9}RRERRVRSR^{17} region is essential for interactions between P7a and importin α, and has dramatic effects on the nuclear localization of P7a (Figs. 3 and 4). Moreover, changes to the ^{9}RR^{10} residues within the motif had a less substantial influence on P7a and importin α interactions than substitutions within ^{12}RRVRSR^{17} (Fig. 4C and E).

3.4. The R-rich motif mediates nucleolar and Cajal bodies targeting

The fluorescence of pGDG-P7a and pGD-RFP-GUS-P7a also appeared to accumulate in sub-nuclear bodies (Figs. 2A and 3A). Therefore, we used the fibrillarin protein, which localizes in the nucleolus and Cajal bodies (CBs) as a sub-nuclear marker to provide more precise evaluation of P7a localization. The *fibrillarin* (Fib) gene was cloned from *N. benthamiana*, fused to the C-terminus of GFP to produce pGDG-Fib, and then co-expressed in *N. benthamiana* leaves with the P7a vectors, pGDR-GUS-P7a, pGDR-GUS-P7a$_{R5A}$, pGDR-GUS-P7a$_{R9A,R10A}$, or pGDR-GUS-P7a$_{R21A,K22A}$. The intense red fluorescence from pGDR-GUS-P7a was visible as large nuclear bodies and as smaller intense foci that co-localized with the green fluorescence from pGDG-Fib. The latter result suggested that P7a was concentrated in the nucleolus and possibly in the CBs (Fig. 5A). The P7a mutant fusion protein, RFP-GUS-P7a$_{R5A}$, also accumulated in the nucleolar (Fig. 5B). However the RFP-GUS-P7a$_{R9A,R10A}$ mutant failed to localize to the nucleolus (Fig. 5C), whereas the separate mutant RFP-GUS-P7a$_{R21A,K22A}$ was similar to P7a in nucleolar targeting (Fig. 5D). When co-infiltration experiments were performed with bacteria harboring pGDG-7a (Fig. 1C) and pGDR-Fib (Fig. 1D), sub-nuclear localization of both proteins was similar to that of RFP-GUS-P7a from pGDR-Gus-P7a (Fig. 5E and data not shown). Interestingly, when a single nucleus contained two nucleoli, the P7a fluorescence was always confined to one nucleolus (Fig. 5E), so it is possible that nucleolar localization functions may target P7a accumulation to specific nucleolar addresses during the early phases of foci formation. Irrespective of this notion, we conclude that the ^{12}RRVRSR^{17} region within the R-rich motif is essential for nuclear localization, whereas the adjacent motif ^{9}RR^{10} functions to specify P7a nucleolar targeting. Furthermore, the amino acid sequence ^{9}RRERRVR^{15} is similar to the signal sequence (R/K)(R/K)X(R/K) previously reported to function in nucleolar localization (Horke et al., 2004; Weber et al., 2000).

Fibrillarin is an important protein of nucleus and CBs. The ORF3 protein of GRV, VPg protein of PVA and the other proteins encoded by animal viruses can interact with the protein fibrillarin (Kim et al., 2007a,b; Rajamaki and Valkonen, 2009). To detect

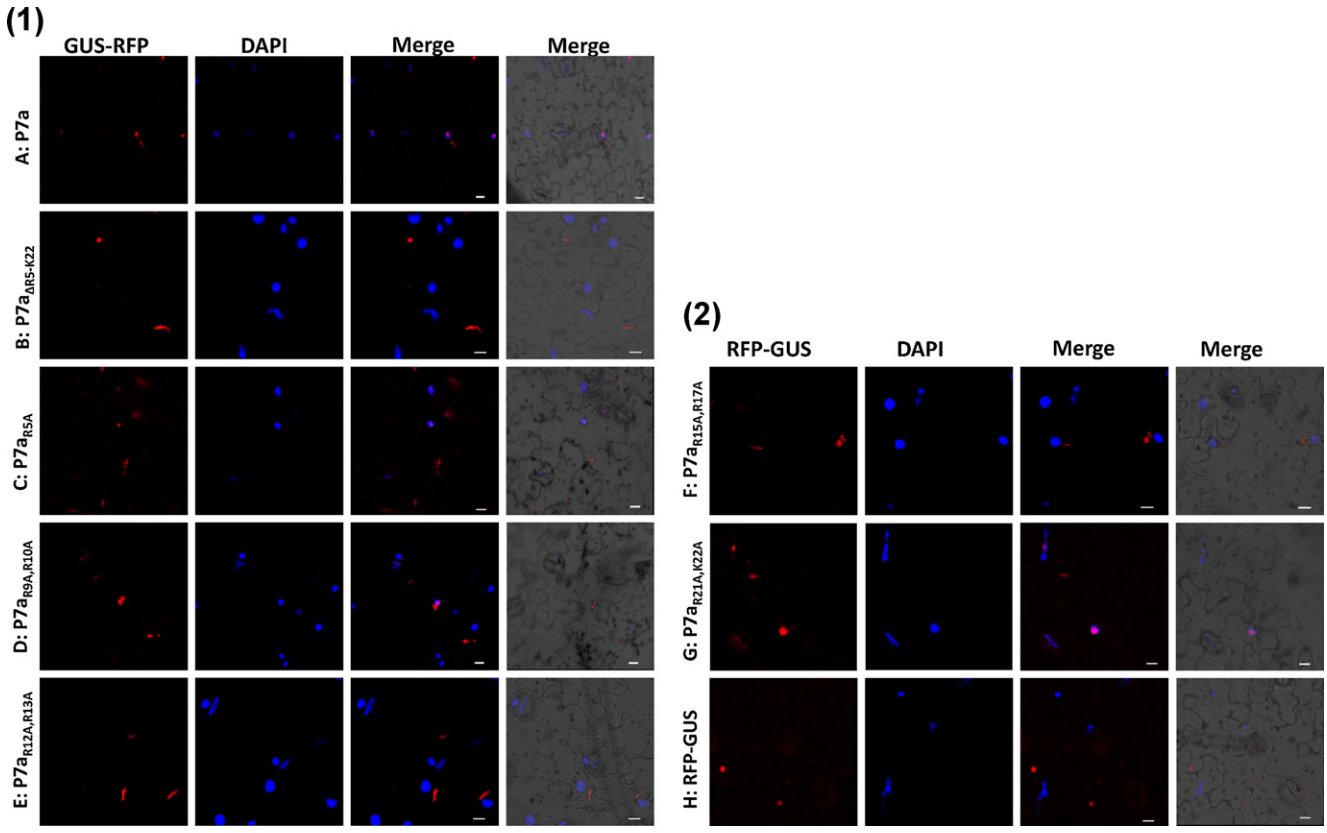

Fig. 3. Subcellular localization of BBSV P7a and P7a mutants in *N. benthamiana* by RFP fluorescence microscopy. Epidermal leaf cells of *N. benthamiana* leaves infiltrated with Agrobacterium containing pGDR-GUS-p7a plasmids harboring wtP7a or P7a mutants. (A) pGDR-GUS-P7a, (B) pGDR-GUS-P7a$_{\Delta R5\text{-}R22}$, (C) pGDR-GUS-P7a$_{R5A}$, (D) pGDR-GUS-P7a$_{R9A,R10A}$, (E) pGDR-GUS-P7a$_{R12A,R13A}$, (F) pGDR-GUS-P7a$_{R15A,R17A}$, (G) pGDR-GUS-P7a$_{R21A,K22A}$, and (H) pGDR-GUS. The images were visualized by DIC microcopy at 2–3 days post-inoculation and DAPI staining (blue) was used to detect nuclei. Bars = 10 μm. (For interpretation of the references to color in this sentence, the reader is referred to the web version of the article.)

possible interaction between fibrillarin and P7a, we again used BiFC assays. In these experiments, leaf cells expressing pYN-Fib and pYC-P7a showed a strong fluorescent signal that appeared to be most intense in the nucleolus and the CBs (Fig. 6A). When the pYC-P7a$_{R5A}$ mutant was tested for interactions with pYN-NbFib, fluorescence was observed only in the nucleolus (Fig. 6B). However, infiltrated leaves including pYC-P7a$_{R21A,K22A}$ and pYN-NbFib, exhibited fluorescence in both the nucleolus and the CBs (Fig. 6C). Furthermore, the *in vitro* far western assay results indicate that the His-labeled P7a was able to bind the fibrillarin which fused to GST-tag (Supplementary material Fig. S1).These results suggest that specific binding interactions between P7a and fibrillarin are required for the nucleolar and CBs targeting.

3.5. Mutations in the P7a R-rich motif affect BBSV viral replication and virulence

The importance of the R-rich motif in the virulence of BBSV was also examined by introducing the P7a mutations into the BBSV infectious cDNA clone. To determine whether the mutants infect viral replication, protoplast infectivity experiments were carried out. For this purpose, RNA transcripts from pUBF52, and the mutants pUBF-P7a$_{R5A}$, pUBF-P7a$_{R9A,R10A}$, pUBF-P7a$_{R12A,R13A}$, pUBF-P7a$_{R15A,R17A}$, pUBF-P7a$_{R21A,K22A}$ and the delectation mutant pUBF-P7a$_{\Delta R5\text{-}K22}$ were transfected by polyethylene glycol mediated uptake of viral RNA into *N. benthamiana* protoplasts. Northern blot analyses were used to determine the levels of viral RNAs from the transfected protoplasts at 18 hpi. The results demonstrated that the mutants pUBF-P7a$_{R5A}$, and pUBF-P7a$_{R9A,R10A}$ accumulated similar levels of viral genomic and subgenomic RNAs as wtBBSV (Fig. 7A). The mutant pUBF-P7a$_{R12A,\ R13A}$ replicated similar level of viral genomic RNAs as wtBBSV, but dramatically reduced the accumulated level of subgenomic RNA2. The pUBF-P7a$_{R15A,R17A}$ mutant had moderately reduced the level of viral RNA replication (Fig. 7A). However, the accumulation of pUBF-P7a$_{R21A,K22A}$ and pUBF-P7a$_{\Delta R5\text{-}K22}$ viral RNA was substantially lower (Fig. 7A). The results suggest that the R-rich motif is important for the viral replication and different amino acids mutants have distinct influence.

To determine whether the mutants affect lesion phenotypes, *C. amaranticolor* was inoculated with *in vitro* transcripts from each of the six mutants (pUBF-P7a$_{R5A}$, P7a$_{R9A,R10A}$, P7a$_{R12A,R13A}$, P7a$_{R15A,R17A}$, P7a$_{R21A,K22A}$ and pUBF-P7a$_{\Delta R5\text{-}K22}$) and the wild-type pUBF52. The wtBBSV and the pUBF-P7a$_{R5A}$ mutant produced aggressive infections with spreading local lesions on infected *C. amaranticolor* leaves and the timing of appearance and sizes of the lesions appeared to be similar after 3–4 days at 18 °C (Fig. 7B). However, the mutant P7a$_{R9A,R10A}$, appeared to be less aggressive and produced visibly smaller spreading lesions than the wtBBSV. Leaves inoculated with these two mutant constructs contained similar levels of viral RNA that was lower than the viral RNA from leaves inoculated with the wtBBSV transcripts (Fig. 7C). The lesions elicited by the P7a$_{R15A,R17A}$ mutant were fewer in number than those of wtBBSV, but appeared to be of about the same size as those of isolated wtBBSV lesions, and viral RNA from leaves infected with the P7a$_{R15A,R17A}$ mutant dramatically reduced (Fig. 7B and C). Conversely, *C. amaranticolor* leaves mechanically inoculated with *in vitro* transcripts from the remaining mutants pUBF-P7a$_{R12A,R13A}$, pUBF-P7a$_{R21A,K22A}$ and pUBF-P7a$_{\Delta R5\text{-}K22}$, failed to develop lesions or show any signs of viral infection for 5 days after inoculation (Fig. 7B). Furthermore, leaves infected with these three mutants

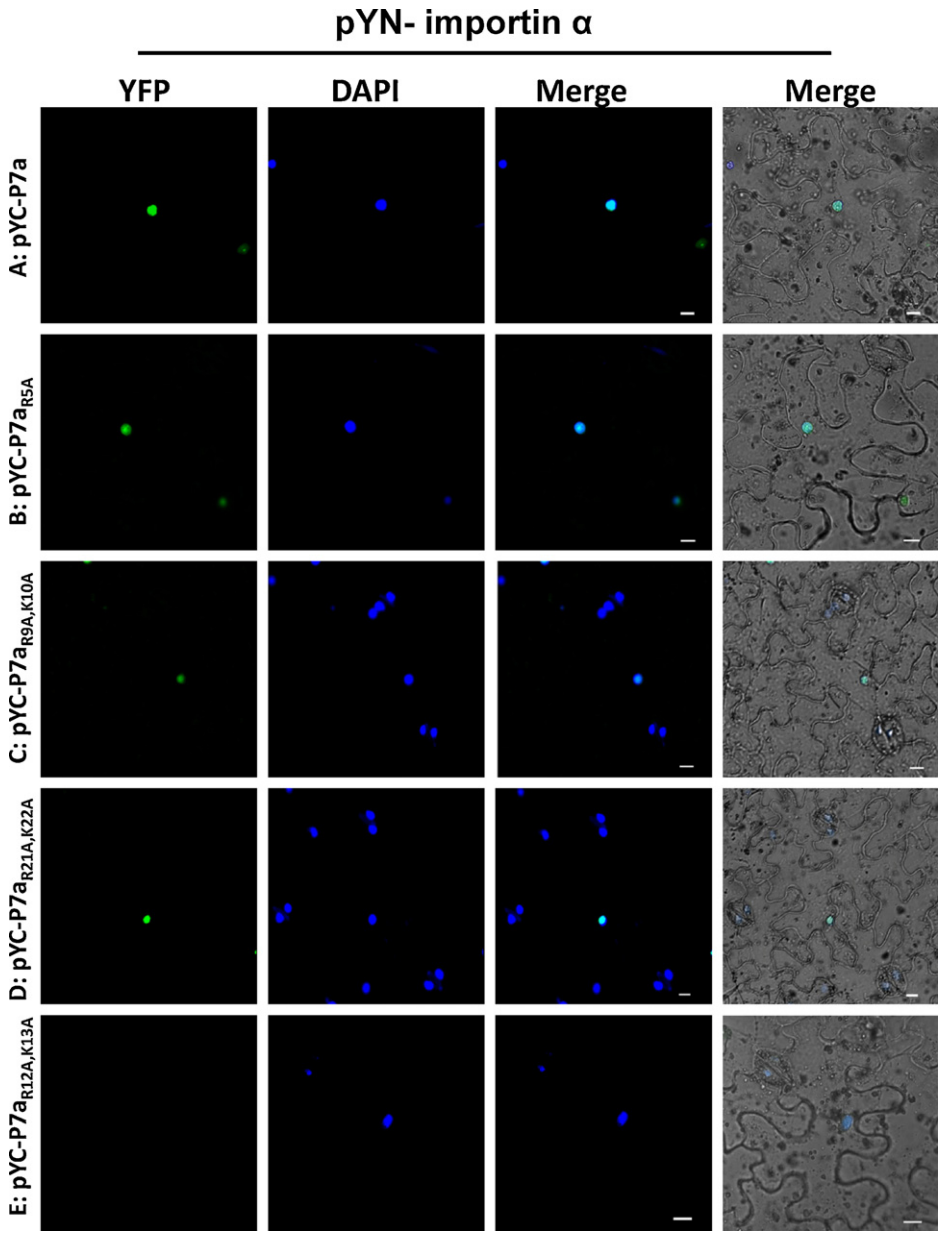

Fig. 4. BiFC assays to assess interactions between the BBSV P7a protein and importin α in the nucleus. Epidermal leaf cells of *N. benthamiana* expressing pYN-importin α and pYC-P7a or pYC-P7a mutants. (A) pYN-importin α and pYC-P7a, (B) pYN-importin α and pYC-P7a$_{R5A}$, (C) pYN-importin α and pYC-P7a$_{R9A,K10A}$, (D) pYN-importin α and pYC-P7a$_{R21A,K22A}$, and (E) pYN-importin α and pYC-P7a$_{R12AR13A}$. The leaf cells expressing pYN-importin α and pYC-P7a$_{R15A,K17A}$, or pYN-importin α and pYC-P7a$_{\Delta R5\text{-}K22}$ failed to exhibit nuclear fluorescence and were otherwise identical to leaf cells agroinfiltrated with pYN-importin α and pYC-P7a$_{R12AR13A}$. Fluorescence images were evaluated by confocal microscopy at 2–3 days after agroinfiltration. Bars = 10 μm.

contained barely detectable levels of viral RNA as detected by northern blot analysis, even when more concentrated preparations of RNA were loaded on the gels (Fig. 7C). Overall, the infectivity results show that mutations on R-rich motif affect plant symptoms and viral replication in plants and protoplasts.

In conclusion, the R-rich motif (^{5}RSEQRRERRVRSRSEDRK^{22}) of P7a determine the nuclear and nucleolar localization, and is important for viral replication and infection. The results indicate that the nuclear localization mutants P7a$_{R5A}$ and P7a$_{R9A,R10A}$ mutants are not compromised substantially in terms of their infection phenotypes and ability to replicate in infected cells. The mutants which abolish targeting nuclear influenced the viral symptom and virus RNA replication in the leaves. The P7a$_{R15A,R17A}$ mutant exhibited reductions in both lesion formation and replication of viral RNA, and the pUBF-P7a$_{R12A,R13A}$, pUBF-P7a$_{\Delta R5\text{-}K22}$ failed to form local lesions or exhibit substantial replication in the leaves. However, the nuclear localization mutant P7a$_{R21A,K22A}$ which produced low level viral RNA in protoplast, also abolished local lesions and dramatically reduced substantial replication.

4. Discussion

Our results show that the nuclear localization of BBSV movement protein is controlled by the R-rich motif of N-terminal. In this study, we have tested Ala-scanning and deletion mutants of P7a R-rich motif in the transient expression assays to further reveal that the motif ^{12}RRVRSR^{17} determined P7a nuclear targeting. In another report of *Turnip crinkle virus*, the cell-to-cell movement P8 protein was localized on the nucleus, suggesting a function in the cell nucleus (Cohen et al., 2000). However, P7a is the first

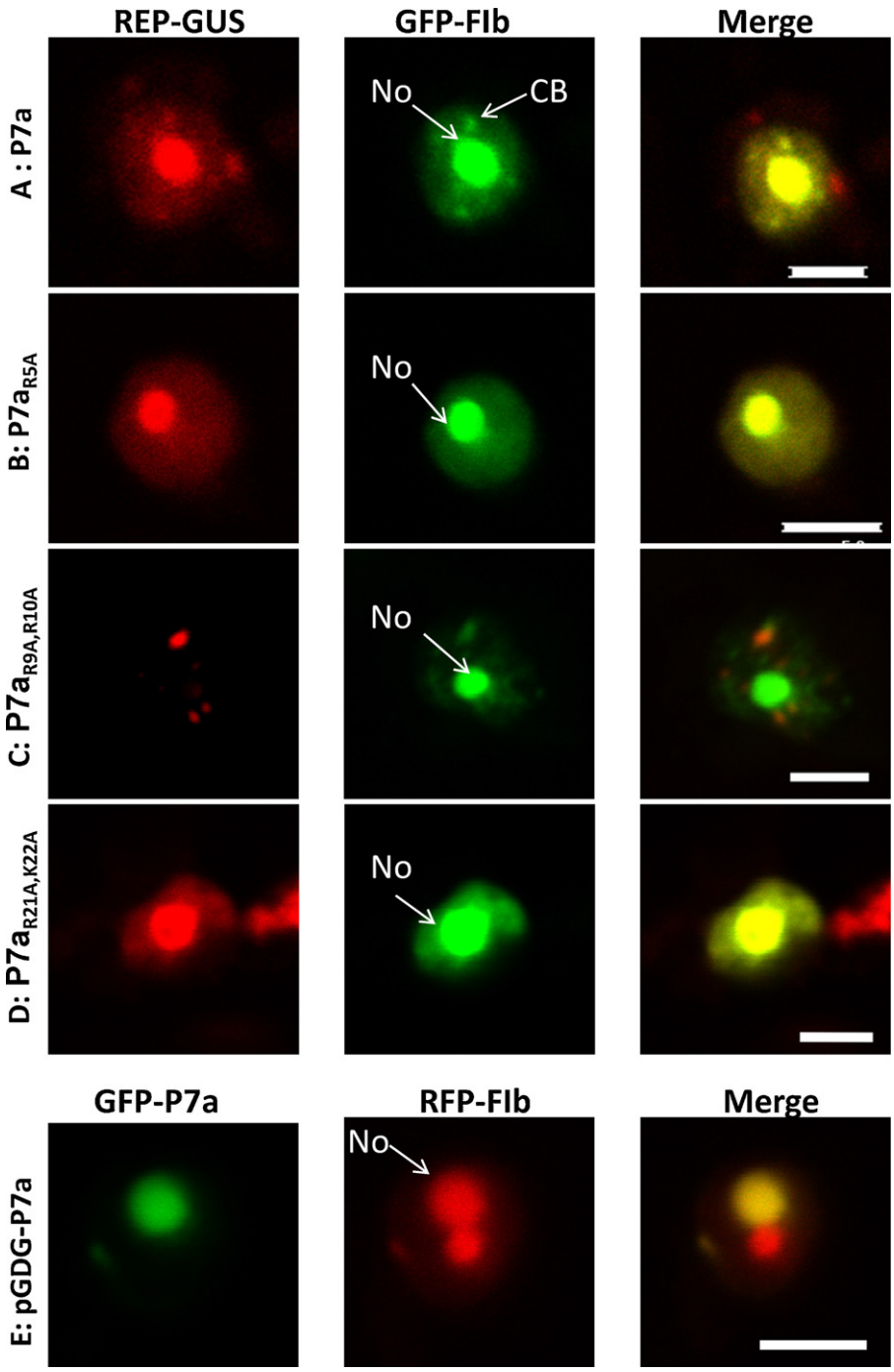

Fig. 5. Subnuclear localization of P7a and mutant fusion proteins by fluorescence microscopy. Epidermal cells of *N. benthamiana* co-infiltrated with pGDG and pGDR binary vectors. (A) pGDG-Fib and pGDR-GUS-P7a, (B) pGDG-Fib and pGDR-GUS-P7a$_{R5A}$, (C) pGDG-Fib and pGDR-GUS-P7a$_{R9A,R10A}$, (D) pGDG-Fib and pGDR-GUS-P7a$_{R21A,K22A}$, (E) pGDR-Fib and pGDG-P7a for fusion protein expression. Images were visualized by confocal microscopy at 2–3 days post-infiltration. The nucleolus (Nu) and Cajal bodies (CBs) are indicated. Bars = 5 μm.

cell-to-cell protein encoded by the *Necrovirus* genus (Lommel et al., 2005) that has been shown to localize in the nuclear. In this study, we further used the BiFC assays to confirm that P7a is targeted to the nucleus also *via* the importin α pathway, the classical import pathway in eukaryotic cells (Lange et al., 2007). Deletion of the R-rich motif abolished P7a associations with importin α, underlying the important role of this region in establishing the interaction. We also found the direct correlation between the nuclear localization of RFP-GUS fusions P7a mutants and interaction of the corresponding P7a versions with the importin α. Many plant virus nuclear proteins always interact with importin α, such as the P25 protein which is encoded by BNYVV, and the CP protein of RTBV(Guerra-Peraza et al., 2005; Vetter et al., 2004). Our evidence also indicates that the R-rich motif of P7a is involved in the P7a nuclear import in an importin α-dependent manner. To predict the nuclear localization possibility of the first movement proteins encoded by the members in the *Necrovirus* genus (Lommel et al., 2005), we used the PSORTII program to analysis the full-length sequences of the proteins. Various scores, such as 52.2% for the P8 protein of *Tobacco necrosis virus* A, 62.2% for the $P7_1$ protein of

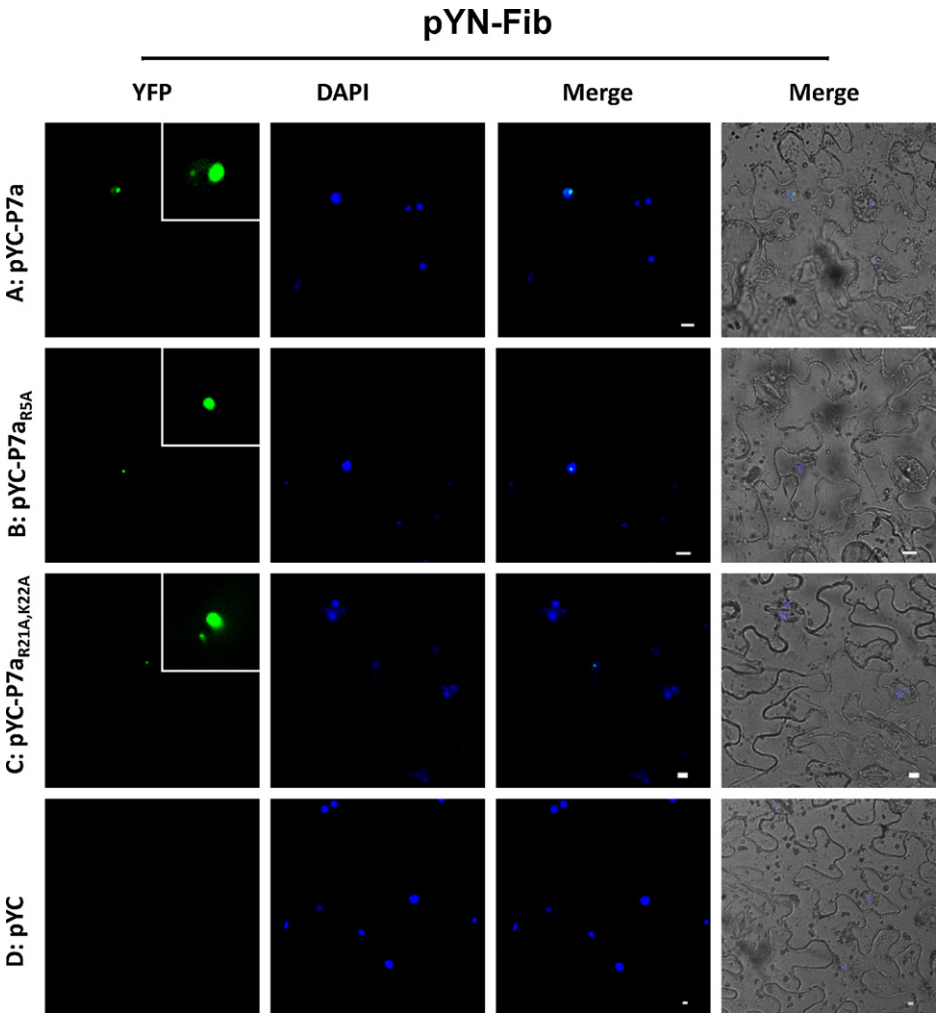

Fig. 6. BiFC assays of nucleolar interactions between BBSV P7a protein and fibrillarin. *N. Benthamiana* epidermal cells co-infiltrated with pYN-Fib and pYC-7a or pYC-7a mutants. (A) pYN-Fib and pYC-P7a, (B) pYN-Fib and pYC-P7a$_{R5A}$, (C) pYN-Fib and pYC-P7a$_{R21A,K22A}$, or (D) pYN-Fib and the pYC binary vector as a control. Fluorescence images were evaluated by confocal microscopy at 2–3 days after infiltration. The images in high magnification (HM) are shown for yellow fluorescence visualization. Bars = 10 μm.

Tobacco necrosis virus D, 43.5% for *Olive latent virus* 1 P8 protein, 34.8% for *Olive latent virus* 1 protein P11, and 60.9% for the P7a protein of BBSV, provide intriguing suggestions that all of these proteins have nuclear localization activity. These results suggest that the nuclear targeting of the first movement protein may be a general phenomenon.

P7a protein was found to accumulate in the nucleolus and CBs. Our results show that ^{9}RRERRVR^{15} of the R-rich motif control the nucleolar targeting. Moreover, the basic residues substitutions of the R-rich motif was sufficient to reduce or interfere with nucleolar localization. Although a few plant RNA virus proteins including protein ORF3 of GRV and the protein VPg of PVA have been observed in the nucleolar and CBs, P7a is the first cell-to-cell movement protein encoded by a plant RNA virus that has been shown to localize in the nucleolus and CBs (Kim et al., 2007a,b; Rajamaki and Valkonen, 2009). Another cell-to-cell movement protein TGB1 encoded by *Potato mop-top virus* was also found in nucleoli (Wright et al., 2010). However, P7a can accumulate in the nucleolar and CBs. As the protein ORF3 of GRV and protein VPg of PVA, the protein P7a interacted with a major nucleolar protein fibrillarin, which is also presented in CBs (Kim et al., 2007a,b; Rajamaki and Valkonen, 2009). However, the interaction between ORF3 protein of GRV and fibrillarin also appears to be required for a nuclear export function involved in recruiting some fibrillarin and ORF3 protein from the nucleus to the cytoplasm (Kim et al., 2007a,b). The nuclear export function is linked to the formation of c-RNPs that are competent for long-distance movement (Kim et al., 2007a,b). BBSV P7a and PVA VPg protein may be distinct functionally from GRV ORF3 protein because the interactions between protein P7a or VPg and fibrillarin were concentrated only in the nucleoli and CBs but not in the cytoplasm. However, the interactions of these viral protein with fibrillarin are important for the viral infection, but the mechanism may be different (Kim et al., 2007a,b; Rajamaki and Valkonen, 2009).

Some available reports show that the nuclear localization protein activity encoded by plant viruses is closely related to the viral symptom severity and virus replication. The viral nuclear localization proteins including P25 encoded by BNYVV and VPg of PVA, are all the symptom and viral replication determinants (Rajamaki and Valkonen, 2009; Vetter et al., 2004). In our experiments, the mutants of the R-rich motif not only influenced the subcellular localization, but also affected symptom phenotype in *C. amaranticolor* and viral replication in protoplast. For example, the mutant P7a$_{R9A,R10A}$, which accumulates in the nucleus but is not imported into the nucleolus, produced fewer and smaller lesions on the leaves than the wild-type virus (Fig. 7B). The mutations, P7a$_{R12A,R13A}$, P7a$_{R15A,R17A}$, and P7a$_{\Delta R5\text{-}K22}$ appeared to abolish the nuclear targeting, produced fewer or no lesions in *C. amaranticolor*, and reduce the viral replication in the protoplast. Since the R-rich motif of P7a has been predicted to have RNA binding capabilities (after using the website http://cubic.bioc.columbia.edu/predictprotein),

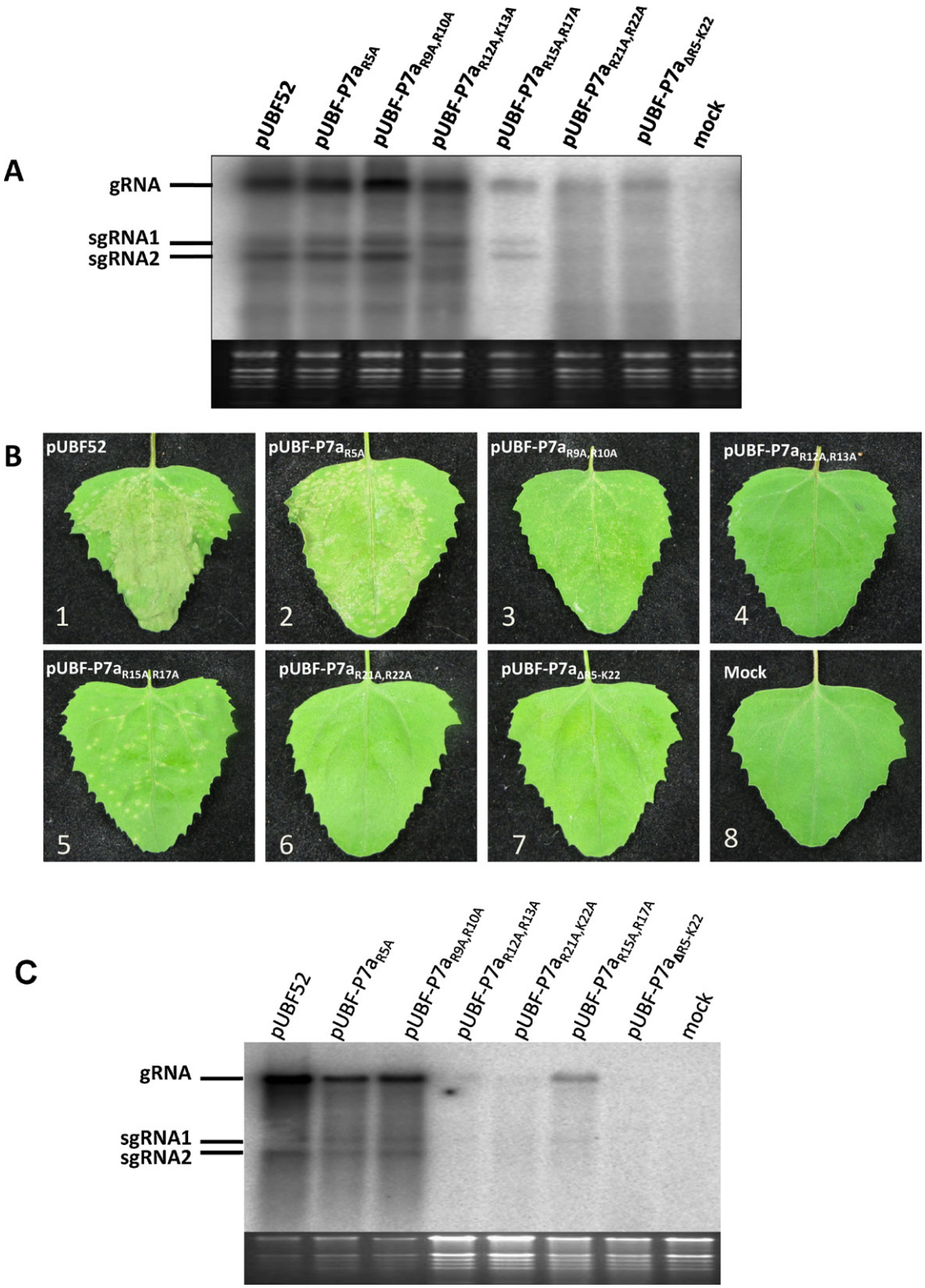

Fig. 7. Infection phenotype and viral replication after inoculation with *in vitro* synthesized RNAs corresponding to wild type BBSV and site-specific BBSV p7a mutants. (A) Northern-blot detection of BBSV RNAs in *N. benthamiana* prototplasts transfected with *in vitro* transcripts from the cDNA clones. Total RNA from inoculated protoplasts was used as a loading control. The electrophoretic mobilities of BBSV genomic RNA (gRNA) and subgenomic RNAs (sgRNA) are indicated on the left. (B) Local lesion responses of *C. amaranticolor* leaves inoculated with RNAs transcribed from pUBF52 cDNA clones. Panels show (1) pUBF52, (2) pUBF-P7a$_{R5A}$, (3) pUBF-P7a$_{R9A,R10A}$, (4) pUBF-P7a$_{R12A,R13A}$, (5) pUBF-P7a$_{R15A,R17A}$, (6) pUBF-P7a$_{R21A,R22A}$, (7) pUBF-P7a$_{\Delta R5-K22}$ (8) Mock. Photos of leaves were taken at 5 days post-inoculation (dpi). (C) Northern-blot detection of RNAs extracted at 5 dpi from *C. amaranticolor* leaves inoculated with the *in vitro* RNA transcripts. Four times as much RNA was loaded on gels from leaves inoculated with pUBF-P7a$_{R12A,R13A}$, pUBF-P7a$_{R15A,R17A}$, pUBF-P7a$_{R21A,K22A}$ and pUBF-P7a$_{\Delta R5-K22}$ transcripts as RNA from leaves inoculated with pUBF52 (wtBBSV), pUBF-P7a$_{R5A}$ and pUBF-P7a$_{R9A,R10A}$ RNA transcripts. Total RNA from mock-inoculated leaves was used as a loading control (Bottom Panel).

we proposed that the mutations on this R-rich motif would not only affect the sub-cellular localization of the protein but also influence its RNA binding activity and consequently cell-to-cell movement. Viral long distance movement of some plant RNA viruses requires nuclear localization. The nucleolar localization of ORF3 protein encoded by GRV and TGB1 protein encoded by PMTV is also essential for the viral long-distance infection (Kim et al., 2007a,b; Wright et al., 2010). Nuclear localization is also required for suppression of gene silencing by some viral proteins (Haas et al., 2008; Rajamaki and Valkonen, 2009). For instance, the P6 protein of *Cauliflower mosaic virus* (CaMV) can localize in the nucleus, interact with DRB4 and suppress gene silencing (Haas et al., 2008). In another case, the PVA NIa–VPg protein is required for the suppression of gene silencing and the initiation of infection and also localizes to the nucleolus and CBs during interactions with the fibrillarin protein (Rajamaki and Valkonen, 2009).

In conclusion, our data demonstrates the viral successful infection cycle involved in the nuclear and nucleolar localization. For some animal viruses like Coronaviruses, the nuclear localization of viral protein is also important for the virus replication and viral infection (Hiscox, 2003; Hiscox et al., 2001; Wurm et al., 2001). Hence, the results may be applicable to the *Necrovirus* genus and some animal viruses.

Acknowledgements

We are grateful to Professor Andrew O. Jackson (Department of Plant and Microbial Biology, University of California at Berkeley) for editing the manuscript and providing the pGDG/pGDR vectors. We also thank Professor Jörg Kudla (Universität Münster, Germany) and Dr. Saskia Hogenhout (John Innes Centre, England) for providing the BiFC vectors and NbImpα1 genes, respectively. This work was supported by the National Natural Science Foundation of China (30730006).

Appendix A. Supplementary data

Supplementary data associated with this article can be found, in the online version, at http://dx.doi.org/10.1016/j.virusres.2012.05.001.

References

Adam, S.A., Geracet, L., 1991. Cytosolic proteins that specifically bind nuclear location signals are receptors for nuclear import. Cell 66 (5), 837–847.
Autonell, C., Ratti, C., Resca, R., De Biaggi, M., Garcia, J., 2006. First report of Beet virus Q in Spain. Plant Disease 90 (1), 110.
Boisvert, F.-M., van Koningsbruggen, S., Navascués, J., Lamond, A.I., 2007. The multifunctional nucleolus. Nature Reviews Molecular Cell Biology 8 (7), 574–586.
Cai, Z.N., Ding, Q., Cao, Y.H., Bo, Y.X., Lesemann, D.E., Jiang, J.X., Koenig, R., Yu, J.L., Liu, Y., 1999. Characterization of a sugar beet (*Beta vulgaris* L.) virus caused black scorch symptom in China, a possible new member of necrovirus. In: Proceedings of the Fourth Symposium of the International Working Group on Plant Viruses with Fungal Vectors, Asilomar Conference Centre, Monterey, California, USA, 5–8 October, pp. 9–12.
Canetta, E., Kim, S.H., Kalinina, N.O., Shaw, J., Adya, A.K., Gillespie, T., Brown, J.W.S., Taliansky, M., 2008. A plant virus movement protein forms ringlike complexes with the major nucleolar protein, fibrillarin, in vitro. Journal of Molecular Biology 376 (4), 932–937.
Canto, T., Uhrig, J.F., Swanson, M., Wright, K.M., MacFarlane, S.A., 2006. Translocation of Tomato Bushy Stunt Virus P19 Protein into the nucleus by ALY proteins compromises its silencing suppressor activity. Journal of Virology 80 (18), 9064–9072.
Cao, Y., Cai, Z., Ding, Q., Li, D., Han, C., Yu, J., Liu, Y., 2002. The complete nucleotide sequence of Beet black scorch virus (BBSV), a new member of the genus Necrovirus. Archives of Virology 147 (12), 2431–2435.
Cao, Y.H., Yuan, X.F., Wang, X.X., Guo, L.H., Cai, Z.N., Han, C.G., Li, D.W., Yu, J.L., 2006. Effect on viral pathogenicity of Beet black scorch virus coat protein. Progress in Biochemistry and Biophysics 33 (2), 127–134.
Cohen, Y., Qu, F., Gisel, A., Morris, T.J., Zambryski, P.C., 2000. Nuclear localization of Turnip crinkle virus movement protein p8. Virology 273 (2), 276–285.
Cronshaw, J.M., Krutchinsky, A.N., Zhang, W., Chait, B.T., Matunis, M.J., 2002. Proteomic analysis of the mammalian nuclear pore complex. The Journal of Cell Biology 158 (5), 915–927.
Gonzalez-Vazquez, M., Ayala, J., Garcia-Arenal, F., Fraile, A., 2009. Occurrence of Beet black scorch virus infecting sugar Beet in Europe. Plant Disease 93 (1), 21–24.
Goodin, M.M., Dietzgen, R.G., Schichnes, D., Ruzin, S., Jackson, A.O., 2002. pGD vectors: versatile tools for the expression of green and red fluorescent protein fusions in agroinfiltrated plant leaves. Plant Journal 31 (3), 375–383.
Greber, U.F., Fassati, A., 2003. Nuclear import of viral DNA genomes. Traffic 4 (3), 136–143.
Guerra-Peraza, O., Kirk, D., Seltzer, V., Veluthambi, K., Schmit, A., Hohn, T., Herzog, E., 2005. Coat proteins of Rice tungro bacilliform virus and Mungbean yellow mosaic virus contain multiple nuclear-localization signals and interact with importin <alpha>. Journal of General Virology 86 (6), 1815–1826.
Haas, G., Azevedo, J., Moissiard, G., Geldreich, A., Himber, C., Bureau, M., Fukuhara, T., Keller, M., Voinnet, O., 2008. Nuclear import of CaMV P6 is required for infection and suppression of the RNA silencing factor DRB4. EMBO Journal 27 (15), 2102–2112.
Hiscox, J.A., 2003. The interaction of animal cytoplasmic RNA viruses with the nucleus to facilitate replication. Virus Research 95 (1–2), 13–22.
Hiscox, J.A., Wurm, T., Wilson, L., Britton, P., Cavanagh, D., Brooks, G., 2001. The coronavirus infectious bronchitis virus nucleoprotein localizes to the nucleolus. Journal of Virology 75 (1), 506–512.
Horke, S., Reumann, K., Schweizer, M., Will, H., Heise, T., 2004. Nuclear trafficking of La protein depends on a newly identified nucleolar localization signal and the ability to bind RNA. Journal of Biological Chemistry 279 (25), 26563–26570.
Jiang, J.X., Zhang, J.F., Che, S.C., Yang, D.J., Yu, J.L., Cai, Z.N., Liu, Y., 1999. Transmission of beet black scorch virus by Olpidium brassicae. Journal of Jiangxi Agricultural University 21, 525–528.
Kalderon, D., Roberts, B.L., Richardson, W.D., Smith, A.E., 1984. A short amino acid sequence able to specify nuclear location. Cell 39 (3), 499–509.
Kanneganti, T.D., Bai, X., Tsai, C.W., Win, J., Meulia, T., Goodin, M., Kamoun, S., Hogenhout, S.A., 2007. A functional genetic assay for nuclear trafficking in plants. Plant Journal 50 (1), 149–158.
Kim, S.H., MacFarlane, S., Kalinina, N.O., Rakitina, D.V., Ryabov, E.V., Gillespie, T., Haupt, S., Brown, J.W.S., Taliansky, M., 2007a. Interaction of a plant virus-encoded protein with the major nucleolar protein fibrillarin is required for systemic virus infection. Proceedings of the National Academy of Sciences of the United States of America 104 (26), 11115–11120.
Kim, S.H., Ryabov, E.V., Kalinina, N.O., Rakitina, D.V., Gillespie, T., MacFarlane, S., Haupt, S., Brown, J.W.S., Taliansky, M., 2007b. Cajal bodies and the nucleolus are required for a plant virus systemic infection. EMBO Journal 26 (8), 2169–2179.
Koenig, R., Valizadeh, J., 2008. Molecular and serological characterization of an Iranian isolate of Beet black scorch virus. Archives of Virology 153 (7), 1397–1400.
Kosugi, S., Hasebe, M., Matsumura, N., Takashima, H., Miyamoto-Sato, E., Tomita, M., Yanagawa, H., 2009. Six classes of nuclear localization signals specific to different binding grooves of importin α. Journal of Biological Chemistry 284 (1), 478–485.
Krichevsky, A., Kozlovsky, S.V., Gafni, Y., Citovsky, V., 2006. Nuclear import and export of plant virus proteins and genomes. Molecular Plant Pathology 7 (2), 131–146.
Lange, A., Mills, R.E., Lange, C.J., Stewart, M., Devine, S.E., Corbett, A.H., 2007. Classical nuclear localization signals: definition, function, and interaction with importin α. Journal of Biological Chemistry 282 (8), 5101–5105.
Lommel, S., Martelli, G., Rubino, L., Russo, M., 2005. Genus Necrovirus. Virus Taxonomy: Classification and Nomenclature of Viruses. Eighth Report of the International Committee on Taxonomy of Viruses. Elsevier Academic Press, San Diego.
Morozov, S.Y., Solovyev, A.G., 2003. Triple gene block: modular design of a multifunctional machine for plant virus movement. Journal of General Virology 84 (6), 1351–1366.
Nagy, J., Maliga, P., 1976. Callus Induction and Plant Regeneration from Mesophyll Protoplasts of Nicotiana sylvestris. Zeitschrift fuer Pflanzenphysiologie, Germany, FR.
Olson, M.O.J., 2004. In: Olson, M.O.J. (Ed.), Nontraditional Roles of the Nucleolus. The Nucleolus. Kluwer/Plenum, New York, pp. 329–342.
Olson, M.O.J., Dundr, M., Szebeni, A., 2000. The nucleolus: an old factory with unexpected capabilities. Trends in Cell Biology 10 (5), 189–196.
Pemberton, L.F., Paschal, B.M., 2005. Mechanisms of receptor-mediated nuclear import and nuclear export. Traffic 6 (3), 187–198.
Pontes, O., Li, C.F., Nunes, P.C., Haag, J., Ream, T., Vitins, A., Jacobsen, S.E., Pikaard, C.S., 2006. The Arabidopsis chromatin-modifying nuclear siRNA pathway involves a nucleolar RNA processing center. Cell 126 (1), 79–92.
Rajamaki, M.-L., Valkonen, J.P.T., 2009. Control of nuclear and nucleolar localization of nuclear inclusion protein a of Picorna-like Potato virus A in nicotiana species. Plant Cell 21 (8), 2485–2502.
Robbins, J., Dilwortht, S.M., Laskey, R.A., Dingwall, C., 1991. Two interdependent basic domains in nucleoplasmin nuclear targeting sequence: identification of a class of bipartite nuclear targeting sequence. Cell 64 (3), 615–623.
Ryabov, E.V., Kim, S.H., Taliansky, M., 2004. Identification of a nuclear localization signal and nuclear export signal of the umbraviral long-distance RNA movement protein. Journal of General Virology 85 (5), 1329–1333.
Truant, R., Cullen, B.R., 1999. The arginine-rich domains present in Human Immunodeficiency Virus Type 1 Tat and Rev function as direct importin beta-dependent nuclear localization signals. Molecular and Cellular Biology 19 (2), 1210–1217.

Uhrig, J.F., Canto, T., Marshall, D., MacFarlane, S.A., 2004. Relocalization of nuclear ALY proteins to the cytoplasm by the Tomato Bushy Stunt Virus P19 pathogenicity protein. Plant Physiology 135 (4), 2411–2423.

Urban, A., Neukirchen, S., Jaeger, K.-E., 1997. A rapid and efficient method for site-directed mutagenesis using one-step overlap extension PCR. Nucleic Acids Research 25 (11), 2227–2228.

Vetter, G., Hily, J., Klein, E., Schmidlin, L., Haas, M., Merkle, T., Gilmer, D., 2004. Nucleo-cytoplasmic shuttling of the beet necrotic yellow vein virus RNA-3-encoded p25 protein. Journal of General Virology 85 (8), 2459–2469.

Walter, M., Chaban, C., Schütze, K., Batistic, O., Weckermann, K., Näke, C., Blazevic, D., Grefen, C., Schumacher, K., Oecking, C., Harter, K., Kudla, J., 2004. Visualization of protein interactions in living plant cells using bimolecular fluorescence complementation. Plant Journal 40 (3), 428–438.

Weber, J.D., Kuo, M.L., Bothner, B., DiGiammarino, E.L., Kriwacki, R.W., Roussel, M.F., Sherr, C.J., 2000. Cooperative signals governing ARF-mdm2 interaction and nucleolar localization of the complex. Molecular and Cellular Biology 20 (7), 2517–2528.

Weiland, J.J., Larson, R.L., Freeman, T.P., Edwards, M.C., 2006. First report of Beet black scorch virus in the United States. Plant Disease 90 (6), 828.

Weis, K., 2003. Regulating access to the genome: nucleocytoplasmic transport throughout the cell cycle. Cell 112 (4), 441–451.

Weis, K., Ryder, U., Lamond, A.I., 1996. The conserved amino-terminal domain of hSRP1 alpha is essential for nuclear protein import. EMBO Journal 15 (8), 1818–1825.

Wright, K.M., Cowan, G.H., Lukhovitskaya, N.I., Tilsner, J., Roberts, A.G., Savenkov, E.I., Torrance, L., 2010. The N-terminal domain of PMTV TGB1 movement protein is required for nucleolar localization, microtubule association, and long-distance movement. Molecular Plant–Microbe Interactions 23 (11), 1486–1497.

Wu, Y.L., Li, Q., Chen, X.-Z., 2007. Detecting protein–protein interactions by far western blotting. Nature Protocols 2 (12), 3278–3284.

Wurm, T., Chen, H., Hodgson, T., Britton, P., Brooks, G., Hiscox, J.A., 2001. Localization to the nucleolus is a common feature of Coronavirus nucleoproteins, and the protein may disrupt host cell division. Journal of Virology 75 (19), 9345–9356.

Yoo, S.-D., Cho, Y.-H., Sheen, J., 2007. Arabidopsis mesophyll protoplasts: a versatile cell system for transient gene expression analysis. Nature Protocols 2 (7), 1565–1572.

Yuan, X.F., Cao, Y.H., Xi, D.H., Guo, L.H., Han C. h. Li, D.W., Zhai, Y.F., Yu, J.L., 2006. Analysis of the subgenomic RNAs and the small open reading frames of Beet black scorch virus. Journal of General Virology 87 (10), 3077–3086.

Zhang, Y.J., Zhang, X.F., Niu, S.F., Han, C.G., Yu, J.L., Li, D.W., 2011. Nuclear localization of Beet black scorch virus capsid protein and its interaction with importin α. Virus Research 155 (1), 307–315.